DOI: 10.1021/ma901513y

Macromolecules
ARTICLE

Parallel-Layer Orientation and Its Instability in Side-Chain Polymer Smectic Liquid Crystals under Shear Flow

Masatoshi Tokita,* Go Sugiyama, Satoshi Masuyama, Toshinari Ishii, Sungmin Kang, and Junji Watanabe

Department of Organic and Polymeric Materials, Tokyo Institute of Technology, Ookayama, Meguro-ku, Tokyo 152-8552, Japan

Received July 13, 2009; Revised Manuscript Received September 14, 2009

ABSTRACT: Smectic layer orientation was investigated for the side-chain PM10ME liquid crystal polymer to which steady shear and large amplitude oscillatory shear (LAOS) flows were applied. Two types of orientation are achieved depending on the shear rate $\dot{\gamma}$ and the frequency ω, both of which are presumed to be inversely proportional to the time scale of shear flow. Parallel orientation with the layer normal in the velocity gradient direction is achieved by steady shear flow at $\dot{\gamma} < 10^{-1}$ s^{-1}, but the layers undulate along the neutral direction. Undulation is eliminated under LAOS flow at $\omega > 10^{1}$ rad s^{-1}, which gives a transparent sample with perfect parallel orientation. Shear flows under other conditions (steady shear at $\dot{\gamma} > 10^{-1}$ s^{-1} and LAOS at $\omega < 10^{1}$ rad s^{-1}) tend to induce perpendicular orientation in which the layer normal points in the neutral direction. These results show that layer orientation changes from parallel to perpendicular and back to parallel with shortening time scale of shear flow. These changes in orientation are explainable if fluctuations, which couple to shear flow to induce perpendicular orientation, are averaged out and suppressed under the longer- and shorter-time scale shear flows.

1. Introduction

Deformation and flow are among the proven processes for providing macroscopically oriented samples of condensed matter such as liquid crystals (LCs) and ordered block copolymer melts. Shear-flow orientations in block copolymer lamellar phases have been frequently studied and characterized by certain common features.[1−8]

There are three types of macroscale orientation (parallel, perpendicular, and transverse) in which layer normal is parallel to the velocity gradient, neutral, and velocity directions, respectively. Which orientation is achieved depends on the relative stability of the layer's distinct well-aligned states. Transverse orientation is least stable because in that orientation, shear flow is always accompanied by high-energy deformations such as layer dilation or compression. If fluctuations on the layered structure couple to shear, parallel orientation becomes less stable and perpendicular orientation becomes more stable.[7,8]

This orientation regime is confined to shear flow that is fast enough so that fluctuations do not average out. Therefore, orientation changes from parallel to perpendicular with increasing shear rate (or frequency). Subsequent reorientation to parallel with further increasing shear rate (or frequency) is sometimes seen. When the shear rate (or frequency) becomes high enough for shear to couple to more local dynamics (such as chain conformation relaxation), the difference in mechanical properties between the two types of polymer segment in the block copolymer drives the modulus of the parallel state to lower than that of the perpendicular state, and the block copolymer reorients to parallel. Therefore, there is now experimental[1−4] and theoretical[5−8] evidence of orientation change in block copolymer lamellar phases under shear flow.

*Corresponding author. Tel: +81-3-5734-2834. Fax: +81-3-5734-2888. E-mail: mtokita@polymer.titech.ac.jp.

Lamellar structures also form in the smectic phases of side-chain liquid crystal polymers (SCLCPs), which consist of mesogens laterally attached to a flexible main chain.[9−17] In contrast with the case of block copolymer lamellar phases, changes in the orientation of SCLCP smectic layers under shear flow have not been reported.

In this study, we have investigated layer orientation in a SCLCP smectic liquid crystal under shear flow. Steady shear flow and large amplitude oscillatory shear (LAOS) flow of the smectic LC induce two types of orientation depending on the shear rate or frequency, which are presumed to be inversely proportional to the time scale of shear flow. Steady shear flow at rates lower than 10^{-2} s^{-1} induces parallel orientation and at rates $>10^{0}$ s^{-1} induces perpendicular orientation. LAOS at frequencies $>10^{1}$ rad s^{-1} induces parallel orientation. Orientation under shear flow thus changes from parallel to perpendicular and back to parallel with shortening time scale of shear flow.

2. Experimental Section

Smectic side-chain PM10ME LC polymer with the following chemical structure was synthesized by atom-transfer radical

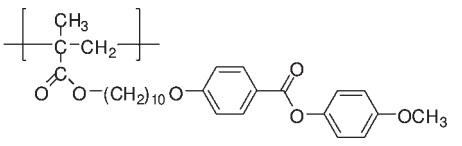

polymerization.[17] The number-averaged molecular weight, M_n, is 22 400 and the dispersity M_w/M_n is 1.34, as determined by gel permeation chromatography using polystyrene as standard. The polymer forms isotropic and then smectic A (SmA) phases with decreasing temperature. SmA LC vitrifies under ordinary conditions. The glass transition and isotropization temperatures

 Published on Web 09/28/2009

of the SmA phase, determined by differential scanning calorimetry (Perkin-Elmer Pyris1 DSC) at a heating rate of 10 °C min^{-1}, are 24 and 117 °C, respectively. Smectic layer spacing is 31.5 Å, roughly equal to the side-chain length (29.5 Å), indicating that the smectic phase type is smectic A_1.

Steady shear flow and LAOS flow were applied to the samples by a rheometer (UBM Rheosol G3000) with cone-and-plate geometry (25 mm diameter, 5.642°) and a rheometer (Anton Paar Physica MCR 300) with parallel-plate geometry (25 mm diameter, 0.50 mm gap), respectively, at different shear rates (or frequencies) and temperatures. The LAOS strain amplitude was set to 100% at the rim of the plate. Prior to each shear flowing, to erase any prior thermal/mechanical history, the sample was heated to the isotropic phase (130 °C), held there for 5 min, and then cooled into the smectic phase at a predetermined temperature, resulting in random polydomain. The shear-flow period was fixed at 2 h, within which the appearing modulus decreases and converges to a constant value. After the shear flow was stopped, the sample was cooled to room temperature at a rate of 10 °C min^{-1} and then removed from the rheometer fixture by putting it into liquid nitrogen.

Orientation of the smectic layer in the sheared samples was determined by wide-angle X-ray diffraction (WAXD) patterns recorded on a flat imaging plate by irradiating graphite monochromated Cu Kα radiation (Rigaku UltraX18) to the film sample in the characteristic velocity-gradient ($\nabla\mathbf{v}$), velocity ($\mathbf{v}$), and vorticity ($\mathbf{v} \times \nabla\mathbf{v}$) directions.[17,18] The samples subjected to LAOS were cut from the disk-shaped film at a radius of 10 mm; therefore, the applied shear strain was 80%. WAXD patterns of the sheared samples show no change in smectic layer spacing.

Steady shear viscosity was measured by a rheometer (Anton Paar Physica MCR 300) with cone-and-plate geometry (10 mm diameter, 1°). Dynamic viscosity was measured by the parallel-plate rheometer described above at strain amplitude increasing from 0.1 to 3% and frequency decreasing from 628 to 0.0628 rad s^{-1}.

3. Results

3.1. Steady Shear Flow Orientation. Smectic melt was subjected to steady shear flow at various rates and temperatures. Figure 1 shows the resulting morphologies as revealed by 2D-WAXD measurements. Two types of smectic layer orientation were obtained. The first type of orientation is parallel, with the layer normal preferentially parallel to the $\nabla\mathbf{v}$ direction (Figure 1a, schematic drawing at bottom). The sample sheared at lower shear rate 1.06×10^{-3} s^{-1} and smectic temperature 80 °C shows smectic layer reflections in the $\nabla\mathbf{v}$ direction of the $\mathbf{v}-\nabla\mathbf{v}$ and $\mathbf{v} \times \nabla\mathbf{v}$ $-\nabla\mathbf{v}$ planes and rather weak reflections in the $\mathbf{v} \times \nabla\mathbf{v}$ direction of the $\mathbf{v}-\mathbf{v} \times \nabla\mathbf{v}$ plane, on which the outer halo, attributed to the averaged lateral distance between neighboring two mesogens within a layer, appears to be isotropic. These patterns are typical of parallel orientation.

The second type of orientation is perpendicular, with the smectic layer normal preferentially parallel to the $\mathbf{v} \times \nabla\mathbf{v}$ direction (Figure 1b, schematic drawing at bottom). The sample sheared at higher shear rate 1.06 s^{-1} and the same smectic temperature (80 °C) shows smectic layer reflections in the $\mathbf{v} \times \nabla\mathbf{v}$ direction of the $\mathbf{v}-\mathbf{v} \times \nabla\mathbf{v}$ and $\nabla\mathbf{v}-\mathbf{v} \times \nabla\mathbf{v}$ planes and rather weak reflections in the $\mathbf{v}-\nabla\mathbf{v}$ plane; the outer halo appears to be isotropic. These patterns are typical of perpendicular orientation.

Figure 2 shows the dependence of the orientation on the temperature and the shear rate. The rate range is limited because very high rate shear induces flow instability or accompanies torque over the mechanical range of the rheometer (2 kg cm^{-1}). Lower rate shear flow induces parallel orientation and higher rate shear flow induces perpendicular orientation. Similar trends have been observed for the smectic liquid crystal of a main-chain BB-5(3-Me) LC polyester subjected to steady shear flow.[18]

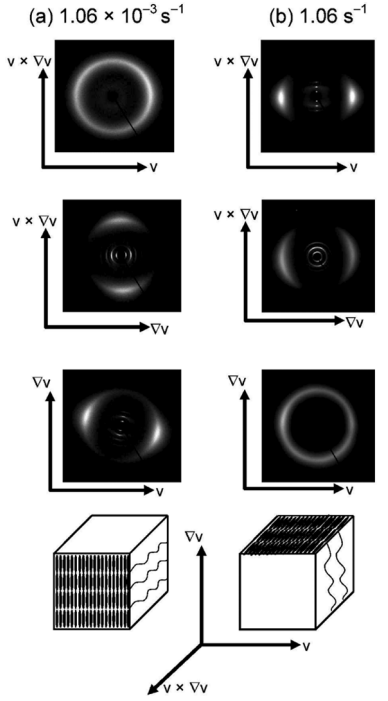

Figure 1. 2D-WAXD results for PM10ME sheared for 2 h at 80 °C with shear rates of (a) 1.06×10^{-3} and (b) 1.06 s^{-1}. Diffraction patterns were measured by irradiating an X-ray beam along three orthogonal directions: velocity ($\mathbf{v}$), velocity gradient ($\nabla\mathbf{v}$), and neutral ($\mathbf{v} \times \nabla\mathbf{v}$). In the insets on the bottom, the resulting orientations are schematically depicted together with the coordinate frame.

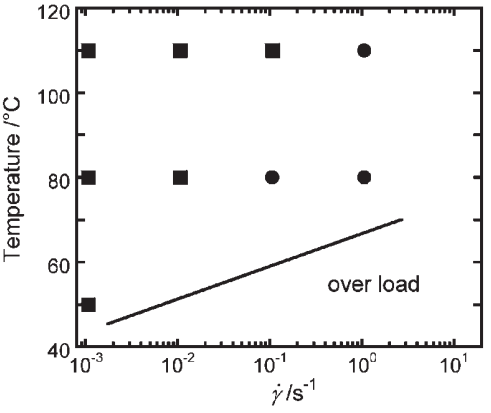

Figure 2. Orientation diagram for layers in the PM10ME smectic LC under steady shear flow. Orientations are parallel (■) or perpendicular (●). Shear rates and temperatures in the lower right were not accessible because the apparent torque was beyond the mechanical range of the rheometer.

3.2. Large Amplitude Oscillatory Shear Flow Orientation. When smectic melt is subjected to oscillatory shear flow with large strain amplitude of 80%, orientation is parallel but becomes disturbed with decreasing LAOS frequency. Figure 3a shows WAXD patterns for a sample sheared at LAOS frequency of $\omega = 106$ rad s^{-1} and smectic temperature of 100 °C. The features of these patterns are similar to those in Figure 1a, except that the layer reflections in the $\nabla\mathbf{v}-\mathbf{v} \times \nabla\mathbf{v}$ plane are not spread azimuthally. These patterns indicate that the smectic layer normal is perfectly parallel to the $\nabla\mathbf{v}$

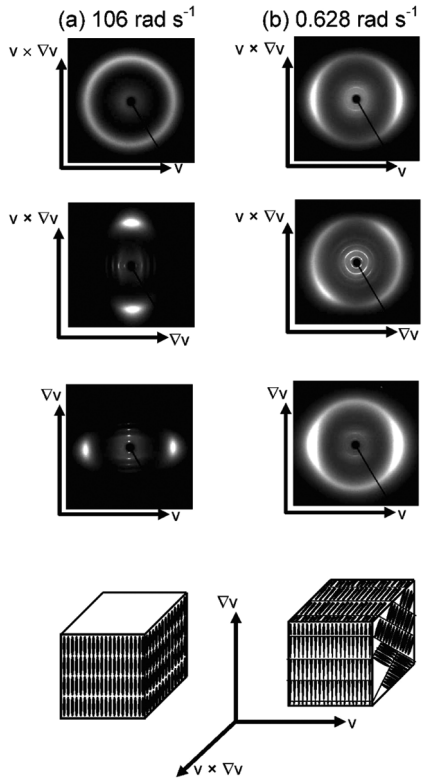

Figure 3. 2D-WAXD results for PM10ME sheared for 2 h at 100 °C with strain amplitude of 80% and frequencies of (a) 106 and (b) 0.628 rad s^{-1}. Diffraction patterns were measured as described in Figure 1.

axis. Also interesting is the fact that the degree of orientation is so high that the sample appears to be transparent.

Layer orientation changes with changing LAOS frequency. Figure 3b shows the WAXD pattern for a sample sheared at lower LAOS frequency of $\omega = 0.628$ rad s^{-1} and the same smectic temperature (100 °C). Smectic layer reflections appear diagonally in the $\mathbf{v} \times \nabla\mathbf{v}$−$\nabla\mathbf{v}$ plane, the $\mathbf{v} \times \nabla\mathbf{v}$ direction of the $\mathbf{v}$−$\mathbf{v} \times \nabla\mathbf{v}$ plane, and the $\nabla\mathbf{v}$ direction of the $\mathbf{v} \times \nabla\mathbf{v}$−$\nabla\mathbf{v}$ plane. These patterns indicate that the smectic layer normal is tilted with respect to the $\nabla\mathbf{v}$ direction of the $\mathbf{v} \times \nabla\mathbf{v}$−$\nabla\mathbf{v}$ plane (Figure 3b, schematic drawing at bottom). We call this type of orientation "nonparallel"; the tilt angle depends on frequency and temperature.

Figure 4 shows the azimuthal angle β of the outer halo maximum, measured clockwise in degrees from the $\mathbf{v} \times \nabla\mathbf{v}$ direction, plotted against LAOS frequency for the various temperatures. β increases toward 90° with decreasing frequency or increasing temperature, which corresponds to perpendicular orientation.

Figure 5 shows the dependence of orientation on temperature and LAOS frequency. Clearly, orientation is parallel at higher frequencies and nonparallel at lower frequencies, and frequency at the orientation boundary decreases with decreasing temperature.

4. Discussion

Our experiments show that the orientation of the smectic layer structure of PM10ME under shear flow depends on the time scale of shear flow. Steady shear flow and LAOS flow under the conditions applied ensure a wide range of flow time scales for smectic melt. The time scales of steady shear flow and LAOS flow are inversely proportional to the shear rate, $\dot{\gamma}$, and frequency, ω, respectively.

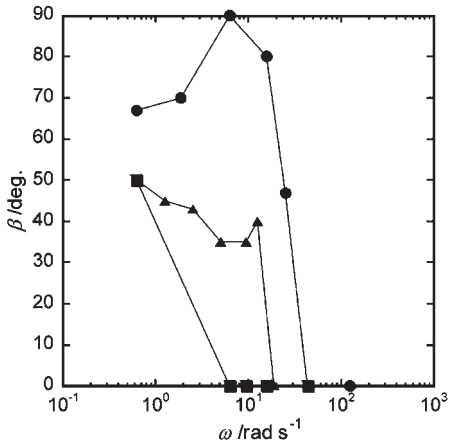

Figure 4. Azimuthal angle β of the outer halo maximum for the WAXD pattern in the $\nabla\mathbf{v}$−$\mathbf{v} \times \nabla\mathbf{v}$ plane plotted against LAOS frequency, ω, measured at the following temperatures: 110 (●), 100 (▲), and 90 °C (■). β is measured clockwise in degrees from the $\mathbf{v} \times \nabla\mathbf{v}$ direction. $\beta = 0$ and 90° corresponds to parallel and perpendicular orientations, respectively.

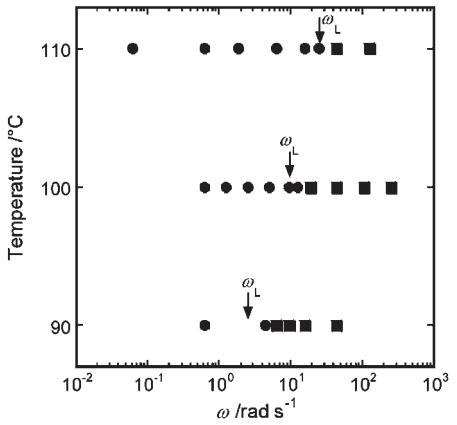

Figure 5. Orientation diagram for the layers in the PM10ME smectic LC under LAOS flow. Orientations are parallel (■) or nonparallel (●). Arrows indicate the characteristic frequency, ω_L, determined by the frequency dependence of the dynamic shear viscosity $|\eta^*|$. (See Figure 7.)

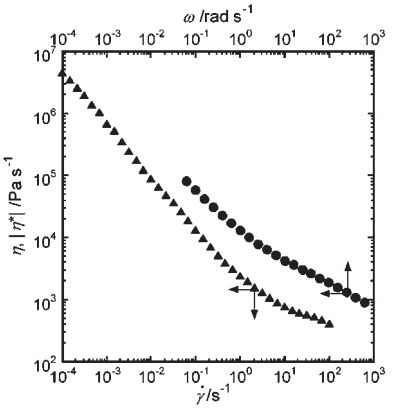

Figure 6. Steady shear (▲) and dynamic viscosities (●) of the PM10ME smectic melt in the polydomain (nonoriented) state measured at 100 °C in cone-and-plate and parallel-plate geometries, respectively.

We can show that $\dot{\gamma}$ and ω can be equated. Figure 6 shows the viscosities at smectic temperature of 100 °C measured by two separate experiments: dynamic shear viscosity, $\eta^*(\omega)$, and steady shear viscosity, $\eta(\dot{\gamma})$. $\eta(\dot{\gamma})$ is significantly smaller than $\eta^*(\omega)$ at

$\dot{\gamma} = \omega$, particularly at high $\dot{\gamma} = \omega$, showing that the empirical Cox−Merz rule[19] equating $\eta^*(\omega)$ with apparent viscosity at the corresponding shear rate $\eta^*(\omega = \dot{\gamma}) = \eta(\dot{\gamma})$ does not appear to hold for the smectic LC. This can be attributed to differences in how strain was applied before measurement. $\eta(\dot{\gamma})$ was measured by increasing $\dot{\gamma}$ stepwise; the applied strain was integrated and increased with increasing $\dot{\gamma}$, which can induce the orientation of the smectic LC to make the apparent viscosity significantly smaller than that measured for the unsheared sample, particularly at high $\dot{\gamma}$. However, the decrease in the apparent viscosity was negligible when $\eta^*(\omega)$ was measured by increasing ω stepwise because it was measured by applying small strain up to 3%.

Except for this disagreement, these two types of viscosity exhibit similar dependence on $\dot{\gamma}$ or ω in the following two respects. First, the trend from extrapolation of $\eta^*(\omega)$ to lower frequency is comparable to that for measured values of $\eta(\dot{\gamma})$. Second, $\eta(\dot{\gamma})$ and $\eta^*(\omega)$ decrease with increasing $\dot{\gamma}$ and ω, respectively, and their rates of decrease become smaller at $\dot{\gamma}$ (or ω) $> 3\ s^{-1}$. These similarities allow us to compare the time scales of steady and oscillatory shear flows by presuming that the time scale of shear flow is inversely proportional to $\dot{\gamma}$ and ω. Coupling the data from Figures 2 and 5, we know that shear flows with time scales longer than 10^1 s and shorter than 10^{-1} s induce parallel orientation, and shear flow with an intermediate time scale induces perpendicular orientation. Our results thus indicate that layer orientation under shear flow changes, with shortening time scale of shear flow, from parallel to perpendicular (that is, nonparallel) and back to parallel.

Such a double flip in layer orientation is explainable by theoretical arguments that attribute parallel-orientation instability to coupling of shear to fluctuations in the layers. Parallel orientation remains stable when fluctuations are either averaged out during deformation or suppressed under shear flow.

The parallel orientation promoted by steady shear flow at a slow rate is explained by averaging out of fluctuations as follows. With parallel orientation, fluctuations are conserved and appear as layer undulation, causing layer reflections in the WAXD pattern to spread in the azimuthal direction. The parallel-oriented sample exhibits such reflection spread in the $\nabla\mathbf{v}-\mathbf{v}\times\nabla\mathbf{v}$ plane rather than the $\mathbf{v}-\nabla\mathbf{v}$ plane (Figure 1a), indicating that undulation remains preferentially in the $\mathbf{v}\times\nabla\mathbf{v}$ direction.[5,6,18] Undulation with the wave vector in the $\mathbf{v}$ direction is also possible but is unfavorable because layers with such undulation suffer high-energy deformations such as layer dilation or compression under shear flow.[5] Parallel orientation induced by slower steady shear flow thus can be explained by assuming that the time scale of shear flow is long enough for fluctuations to be averaged out and conserved preferentially in the $\mathbf{v}\times\nabla\mathbf{v}$ direction. This explanation assumes that fluctuations cannot be averaged out under faster steady shear flow to promote perpendicular orientation, which agrees well with the result shown in Figure 1b.

In contrast, parallel orientation under LAOS flow at high frequency is attributed to the suppression of fluctuations. As shown in Figure 3c, the WAXD patterns of parallel-oriented layers include sharp reflections significantly concentrated in the $\nabla\mathbf{v}$ direction in both the $\mathbf{v}-\nabla\mathbf{v}$ and $\nabla\mathbf{v}-\mathbf{v}\times\nabla\mathbf{v}$ planes, indicating that undulation here is completely eliminated. This undulation elimination in the parallel-oriented sample suggests that high-frequency LAOS flow suppress fluctuations to induce parallel orientation without undulation. This explanation assumes that fluctuations cannot be suppressed under lower-frequency LAOS flow to destabilize parallel orientation, which agrees well with the result shown in Figure 3b.

Note that the frequency regimes for layer orientation under LAOS (Figure 5) can be connected to that for the dynamic shear viscosity $|\eta^*|$. Figure 7 shows the frequency dependence of $|\eta^*|$ for the polydomain sample for the various temperatures. The

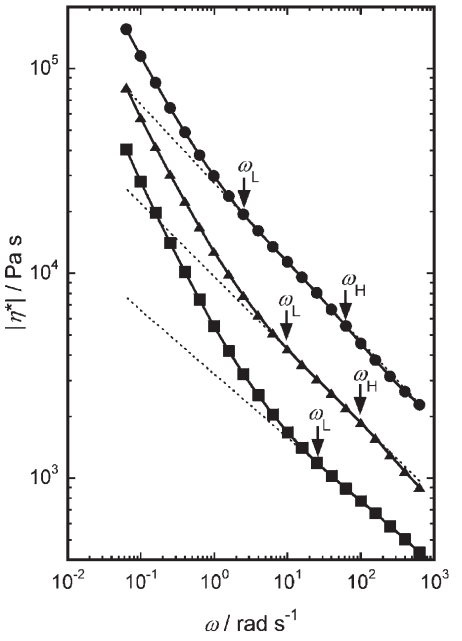

Figure 7. Dynamic viscosity of the PM10ME smectic melt in the polydomain (nonoriented) state measured in parallel-plate geometry at the following temperatures: 90 (●), 100 (▲), and 110 °C (■).

curve of $|\eta^*|$ indicates the existence of three distinct frequency regimes: a central regime of relatively moderate slope (dashed line) and two regimes of larger slope at higher and lower frequencies. Two critical frequencies, ω_L and ω_H, mark the lower and upper frequency bounds of the central regime. In Figure 5, ω_L is denoted by an arrow. Interestingly, ω_L locates the vicinity of the frequency at the boundary between the two orientation regimes (ω_b), indicating that the two types of layer orientation fall in different regimes of the dynamic shear viscosity. ω_b is 1.5 to 2 times higher than ω_L, possibly because of the difference in strain applied for measurements of $|\eta^*|$ (< 3%) and LAOS alignment (80%). This good correspondence between ω_b and ω_L allows us to estimate ω_b from the dynamic viscosity measurement and associates the steeper frequency dependence of $|\eta^*|$ at $\omega < \omega_L$ with layer fluctuations.[20] The other regime with a larger slope at $\omega > \omega_H$ may be attributed to local motion of the molecules. The flow curve (dependence of viscosity on shear rate) shows no trace of parallel-orientation instability under steady shear flow with increasing shear rate.

Parallel-orientation instability under lower-frequency LAOS flow can be evaluated quantitatively by the rotation angle β of the WAXD pattern in the $\mathbf{v}\times\nabla\mathbf{v}-\nabla\mathbf{v}$ plane (Figure 3b). $\beta = 0$ and 90° correspond to parallel and perpendicular orientations, respectively. β increases with decreasing frequency and increasing temperature (Figure 4). These data suggest that higher-frequency fluctuations associated with higher ω_b at higher temperatures can induce stronger undulation instability. However, instability may also be related to the type of flow (LAOS or steady shear). The smectic LC at the same temperature under steady shear flow with longer time scale achieves perpendicular orientation, which suggests that steady shear flow destabilizes parallel orientation more than that by LAOS flow. More detailed investigation is needed to determine the factors governing parallel-orientation instability under shear flow.

As far as we know, this is the first observation of a double flip in layer orientation for the side-chain polymer smectic LC under shear flow. The combination of steady shear and LAOS ensures that the range in shear-flow time scale is wide enough to identify two ranges of parallel orientation at long- and short-time scale shear flows. Intuitively, the SCLCP smectic phase favors parallel

over perpendicular orientations under shear flow. A characteristic of the SCLCP smectic structure is that the mesogens packed in a layer are connected to the main chains on either side of the layer. Both main chain and spacer assume a mostly stretched conformation, so the mesogens should flow at the same velocity to the connected main chain. When the layer has parallel orientation, the layer normal is parallel to the $\nabla \mathbf{v}$ direction, so the main chains on the opposite sides of the layer flow at different velocities, and the layer accommodates the mesogens flowing parallel to the layer at different velocity, enabled by liquid-like packing of mesogens within a layer. Therefore, the smectic layers can fit readily to the velocity gradient under shear flow.

Finally, note that our observation of parallel orientation in the smectic SCLCP is inconsistent with previous observations, indicating preferential perpendicular orientation under steady or LAOS flow. The inconsistency may be due to differences in SCLCP molecular weights. Most of the previous studies examined SCLCPs with high molecular weights of $>50\,000$. Preference for perpendicular orientation has been considered to be promoted by connectivity between layers because of the main-chain backbone passing through the multiple layers expected for high-molecular-weight SCLCPs because the sufficiently long main chain is expected to resist entropy reduction because of the confinement between smectic layers by layer hopping.[21,22] It is supported by the fact that the parallel orientation has been observed not only for polymers with low molecular weights of $\sim 25\,000$,[14] comparable to the sample used (22 400) but also for SCLCPs with high molecular weights $\sim 150\,000$ for which layer hopping is not expected from their small radius of gyration in the layer normal direction measured by small-angle neutron scattering data.[10,11] Perpendicular orientation was reported for polymers with low molecular weights of $\sim 10\,000$ that can be assumed to be too low for layer hopping.[12] This perpendicular orientation can be attributed to coupling of shear flow to fluctuations. Perpendicular orientations of SCLCP smectic layers so far reported are thus attributed to coupling of shear flow to fluctuations or connectivity between layers because of layer hopping. Layer orientations of smectic SCLCPs need to be investigated under shear flows with wide-ranged time scales for polymers with molecular weights over a wide range.

5. Conclusions

Parallel-layer orientation and its instability have been observed for the smectic melt of the side-chain PM10ME LC polymer under steady shear and LAOS flow. Parallel orientation is favored under steady shear flow at $\dot{\gamma} < 10^{-1}\ \mathrm{s}^{-1}$ and LAOS flow at $\omega > 10^{1}\ \mathrm{rad\ s}^{-1}$; under other conditions, it becomes unfavorable and perpendicular orientation becomes more favorable. Although parallel-oriented layers under steady shear flow remain undulated in the $\mathbf{v} \times \nabla \mathbf{v}$ direction, layer undulation is completely eliminated under LAOS flow, and the sample becomes transparent. This indicates that steady shear flow conserves and LAOS flow suppresses undulation fluctuations. Steady shear viscosity and dynamic viscosity depend on $\dot{\gamma}$ and ω, respectively, suggesting that $\dot{\gamma}$ and ω are both inversely proportional to the time scale of shear flow. These results indicate that smectic layer orientation changes, with shortening of the shear time scale, from parallel to perpendicular (or nonparallel) and back to parallel. Parallel orientation is preferred under shear flow with time scales shorter than 10^{-1} s and longer than 10^{1} s, and perpendicular orientation is preferred under shear flow with the intermediate time scale. This behavior is explainable if fluctuations that destabilize parallel orientation by coupling to shear flow are averaged out and suppressed under the longer and shorter time scale shear flows.

Acknowledgment. This research was supported by a Grant-in-Aid for Creative Scientific Research from the Ministry of Education, Science, Sports and Culture, Japan.

References and Notes

(1) Koppi, K. A.; Tirrell, M.; Bates, F. S.; Almdal, K.; Colby, R. H. *J. Phys. II* **1992**, *2*, 1941–1959.
(2) Zhang, Y.; Wiesner, U.; Spiss, H. W. *Macromolecules* **1995**, *28*, 778–781.
(3) Leist, H.; Maring, D.; Thum-Albrecht, T.; Wiesner, U. *J. Chem. Phys.* **1999**, *110*, 8225–8228.
(4) Chen, Z.; Kornfield, J. A.; Smith, S. D.; Grothaus, J. T.; Satkowski, M. M. *Science* **1997**, *277*, 1248–1253.
(5) Bruinsma, R.; Rabin, Y. *Phys. Rev. A.* **1992**, *45*, 994–1008.
(6) Auernhammer, G. K.; Brand, H. R.; Pleiner, H. *Rheol. Acta* **2000**, *39*, 215–222.
(7) Goualian, M.; Milner, S. T. *Phys. Rev. Lett.* **1995**, *74*, 1775–1778.
(8) Fredrickson, G. H. *J. Rheol.* **1994**, *38*, 1045–1067.
(9) Kannan, R. M.; Kornfield, J. A.; Schwenk, N.; Boeffel, C. *Adv. Mater.* **1994**, *6*, 214–216.
(10) Noirez, L.; Lapp, A. *Phys. Rev. E.* **1996**, *53*, 6115–6120.
(11) Noiretz, L.; Lapp, A. *Phys. Rev. Lett.* **1997**, *78*, 70–73.
(12) Wiberg, G.; Skytt, M. −L.; Gedde, U. W. *Polymer* **1998**, *39*, 2983–2986.
(13) Hamley, I. W.; Davidson, P.; Gleeson, A. J. *Polymer* **1999**, *40*, 3599–3603.
(14) Noirez, L. *Phys. Rev. Lett.* **2000**, *84*, 2164–2167.
(15) Auad, M. L.; Kempe, M. D.; Kornfield, J. A.; Rendon, S.; Burghardt, W. R.; Yoon, K. *Macromolecules* **2005**, *38*, 6946–6953.
(16) Rendon, S.; Burghardt, W. R.; Auad, M. L.; Kornfield, J. A. *Macromolecules* **2007**, *40*, 6624–6630.
(17) Tokita, M.; Adachi, M.; Masuyama, S.; Takazawa, F.; Watanabe, J. *Macromolecules* **2007**, *40*, 7276–7282.
(18) Tokita, M.; Tokunaga, K.; Funaoka, S.; Osada, K.; Watanabe, J. *Macromolecules* **2004**, *37*, 2527–2531.
(19) Cox, W. P.; Merz, E. H. *J. Polym. Sci.* **1958**, *28*, 619–622.
(20) Ramaswamy, S. *Phys. Rev. A* **1984**, *29*, 1506–1513.
(21) Renz, W.; Warner, M. *Phys. Rev. Lett.* **1986**, *56*, 1268–1271.
(22) Noirez, L.; Boeffel, C.; Daoud-Aladine, A. *Phys. Rev. Lett.* **1998**, *80*, 1453–1456.